Original Research Article

Evaluating Soil Erosion through Geospatial Techniques: Difficulties and Prospects in the Context of the Central Indian Chambal River Basin

ABSTRACT

Soil erosion is the greatest threat to the ecosystem which gets accelerated due to environmental agents such as water and wind as well as anthropogenic activities. Effective estimation of soil degradation plays an important role in planning preventive measures and conserving the soil. This study was carried out to provide decision-makers with a picture of soil erosion in Madhya Pradesh's Chambal basin and to identify environmentally hot areas to assist in planning effective conservation measures. By using a few input parameters to create raster maps of the Rainfall erosivity factor (R), Soil erodibility factor (K), Topographic factor (LS), Cover and management factor (C), and Support practice factor (P), the Universal Soil Loss Equation (USLE) and Revised Universal Soil Loss Equation (RUSLE) models were applied. The classification of soil erosion and the area portion in each class was then acknowledged. According to the USLE and RUSLE models, the average soil loss for the entire basin is 2.00 t ha-1 yr-1 and 3.04 t ha-1 yr-1, respectively. According to the USLE and RUSLE models, the ranges under severe risk are 0.33% and 0.76%, while the ranges under extremely severe risk are 0.45% and 0.78%, respectively. The land use/land cover (LULC) map for the study area was acquired from satellite data in the USLE, and the Normalized Difference Vegetation Index (NDVI) map was incorporated into the RUSLE model to enhance the comprehension and identification of vegetation. This integration is crucial for capturing detailed information in the RUSLE model. Consequently, RUSLE yields superior results compared to the USLE model, underscoring the significance of incorporating finer details, especially those related to vegetation, for more accurate outcomes.

Keywords: *Soil erosion, Universal Soil Loss Equation, remote sensing, revised universal soil loss equation, conservation planning.*

1. INTRODUCTION

Soil and crop health is a prominent factor and the foundation of agriculture to ensure crop productivity and food security across the globe in the 21st century (Marcinkowski *et al.,* 2022; Khose et al., 2022). Proper growth of the crops and soil moisture management depends upon the available soil properties (Khose et al., 2021; Khose and Mailapalli, 2023; Khose et al., 2023b). It is an indispensable part of the ecosystem that upholds and sustains terrestrial ecosystem services. Soil erosion caused by agents such as water and wind has been a major threat since the beginning of human civilization. In the Anthropocene, it has been further intensified due to human interventions and injudicious agricultural activities (Amundson *et al*., 2015).

Soil is one of the most crucial natural resources that supports human life on earth. It encompasses the entire ecosystem depicting the quality of the soil, water, vegetation, and wildlife. Degradation refers to the land's loss of either temporary or

long-term productive capacity. The IPCC report from 2022 states that "land degradation is the negative trend of the land condition, and due to such degradation soil productivity and soil nutrition are lost and the productive land is turned into wasteland." According to Senapati and Das (2020),the estimated cost of land degradation in India is equal to 3.95% of AGDP and 1.40% of GDP. These studies demonstrate that land degradation is a significant environmental issue everywhere, including India. Therefore, numerous scientists, organizations, and researchers are focusing on environmental degradation and trying to figure out how to stop the degradation of the land (ISRO, 2016; IPCC, 2017).

“In terms of global scale, 1094 million hectares (Mha) of land is affected due to water erosion, out of which 751 Mha being severely harmed. This makes soil erosion the major factor of land degradation. Wind erosion affects 549 Mha of land, with 296 Mha suffering severe effects” (Lal, R., 2003). “An estimated 120.4 Mha of India's 329 Mha total geographical area has been degraded (68% due to water erosion), causing an annual loss of 5.3 Gt of soil. About one-third of the territory in India's Eastern Himalayan region has been damaged by soil erosion brought on by water” (Maji, A. K.,2010). “With an average soil detachment rate of 16.4 t. ha-1. yr-1, out of India's whole geographical region (328.7 Mha), 106 Mha are severely eroding” (Patil *et al*., 2017). “Estimates indicate that 61% of the soil that is eroded is displaced from its original place, 10% is collected in reservoirs, and 29% is completely lost to the sea” (Kar S.K. 2022).

Anthropogenic activities in addition to natural processes enhance land degradation, these processes are also complex and site specific. The socio-economic implication of land degradation can be attributed to continuous loss of agricultural land, decreasing agricultural productivity, worsening food security, and slowereconomic activity which results in low standards of living and poor health status (Pani P and Carling P, 2013). The study found that erosion causes both on-site and off-site losses of soil structure, organic matter, and productivity, as well as low agricultural yields and losses of income. Because of the off-site effects of soil erosion, which decrease the capacity of streams, rivers, and reservoirs and raise the risk of flooding, there is an increase in pollution and sedimentation in downstream areas and rivers. Waterways may continue to be blocked, which could have an impact on the water's quality (Sakinatu I and Ashraf M A, 2017).

Information on a region's spatial and quantitative soil erosion helps with erosion control and agricultural conservation planning. It will aid natural resource conservators and planners to concentrate on the areas that fall under the category of soil erosion severity and plan mitigation measures. In evaluating soil erosion research, the use of remote sensing and geographic information systems (GIS) is highly beneficial since it enables evaluation of spatial heterogeneity in soil, land use/land cover, elevation/slope, etc. Remote sensing can be used to create the input parameters for models of soil erosion (Biswas, 2012). To better understand and forecast outcomes to reduce the detrimental effects of erosion and sedimentation, GIS-based analysis plays a significant role in integrating observations with models (Mitasova *et al*., 2013).

A comparative research study was carried out by Mondal *et al*. (2016) to assess “the soil loss using MMF (Morgan, Morgan and Finney, 1984), USLE, and RUSLE model in a small catchment of the Narmada basin of Madhya Pradesh in central India”. “The differences in the results from the detected data of sedimentation using MMF, USLE, and RUSLE were observed to be (–) 39.45 %, (–) 9.60 %, and 4.80 %, respectively. Therefore, it was concluded that the RUSLE model was more reliable for the study area as compared with the other models”. [49]“The image from January month performed best with overall accuracy of 87% and 0.69 kappa coefficient. This method opens the possibility of using semi-automatic classification for the Chambal badlands which are so far mapped with manual interpretations only” (V. Ranga, 2015). “The average annual soil erosion for the entire state as obtained from the USLE and RUSLE model was 5.80 t. ha-1. yr-1 and 6.64 t. ha-1. yr-1, respectively. The areas under severe risk were 1.09 % and 1.80 %, and very severe risk areas were 1.57 % and 1.83 % as estimated by USLE and RUSLE model, respectively. As compared to RUSLE model, USLE model underestimated rate of soil erosion for most river basins as well as for the entire state” (Suryawanshi, A., 2021).

In rural India, detecting ecologically challenged zones on a regional basis is helpful to create appropriate protection measures. Natural resource management and conservation activities are the primary areas under several employment generation initiatives. The main goal of the current study was to understand the soil erosion process, estimate soil erosion in Chambal basin of Madhya Pradesh using USLE and RUSLE in integration of geospatial technology and compare soil erosion rate estimated using these two models for adaptation of suitable models that can be used to identify environmentally disturbed hot spots and basins aimed at soil protection measures.

2. STUDY AREA

The study region is the second-largest river basin in the Madhya Pradesh state of India. It lies between geographical coordinates of latitudes 22°26'N and 26°54'N and longitudes 74°42' to 79°15'. Forming a geographic boundary between the states of Madhya Pradesh and Rajasthan, it travels from Janapav valley at Malwa Ridge Cows to join the trunk river (Yamuna) in Uttar Pradesh (Kaushik and Ghosh, 2015). Chambal in Madhya Pradesh has a total catchment area of 59,940 sq km. The river Chambal has a total length of 965 km, of which its initial 320 km are in Madhya Pradesh. Its

principal tributaries include the rivers Kali Sindh, Parvati, Kuno, Newaj, and Shipra. The Chambal region experiences humid to sub-humid weather conditions with 900 mm of yearly rainfall (Joshi, 2014). The river flows through a region with diverse geology consisting of igneous, metamorphic, and sedimentary rocks. The river basin is characterized by low to moderate relief, with hills and plateaus of sandstones, shale, and conglomerates. The river and its tributaries have carved deep gorges and valleys through the rocky terrain, creating a unique landscape supporting rich biodiversity. The river is also subject to periodic droughts, which can lead to low flow and increased vulnerability to sand mining. The study area for illegal sand mining comprises sand mining sites that were selected based on reports submitted by the Director of the National Chambal Sanctuary (NCS) and an Additional Director (Mines) to the National Green Tribunal (National Chambal Sanctuary Stretch, 2022). The three primary seasons of the study area's climate are summer, rainy season, and winter. The winter season lasts from October to February, the summer season lasts from March to June, and Köppen–Geiger classification (Kottek *et al*. 2006).

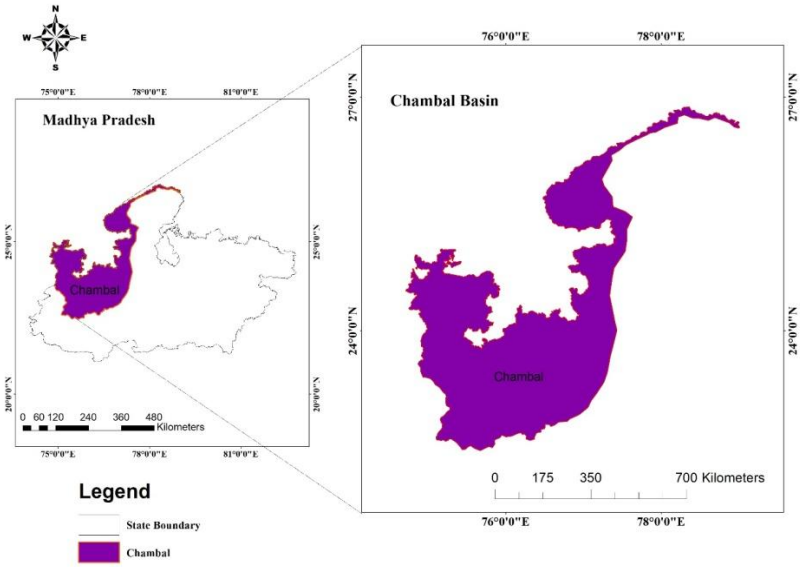

Fig. 1: Location map of the study area.

Clay loam, sandy clay Sandy loam clay, and Sandy loam clay are the major soils available in this basin (Suryawanshi, A., 2021). The Location map of the study area in Madhya Pradesh is depicted in Fig. 1.

2.1 Data Acquisition and Software

In the data collection and analysis process, a varying range of datasets were sourced such as meteorological parameters, soil type, basin characteristics, and land cover data, from various open-access platforms. Detailed information about the data and their specifications can be found in Table 1.

Table 1. Details of various data utilized in this research and their sources

Sl. No.	Data	Data resolution	Source of data
1.	Total rainfall amount	CHIRPS-2.0 (Resolution $0.05^{0)}$	Climate Hazards Group Infrared Precipitation with Station (www.legacy.chg.ucsb.edu/data/chirps/index.html)
2.	NDVI	eMODIS image (250m resolution)	National Aeronautics and Space Administration's (NASA),(http://www.usgs.gov)
3.	Land use	MODIS (Moderate Resolution Imaging Spectroradiometer) image format with (30 m resolution)	National Aeronautics and Space Administration's (NASA), (http://www.usgs.gov)
4.	Soil type	DSMW at scale 1:5 million.	Digital Soil Map of the World, FAO (www.fao.org)
5.	LS and Slope	DEM (30m resolution)	Shuttle Radar TerrainMapper (SRTM), (http://www.usgs.gov)

For meteorological parameter data from the Climate Hazards Group Infrared Precipitation with Station (CHIRPS), datasets were used instead of the India Meteorological Department (IMD) datasets. The CHIRPS datasets offer a higher

spatial resolution of 0.05 × 0.05 degrees, which is more refined compared to the 0.25 × 0.25-degree resolution of the IMD datasets, thanks to their gridded data structure (Prakash, 2019). To process and analyze this data, we employed QGIS version 3.4. This software played a vital role in creating various thematic maps and performing calculations for different parameters. The LULC (land use and land cover) pattern, topography (DEM maps),slope (%) and soil types of the study are depicted in Fig. 2

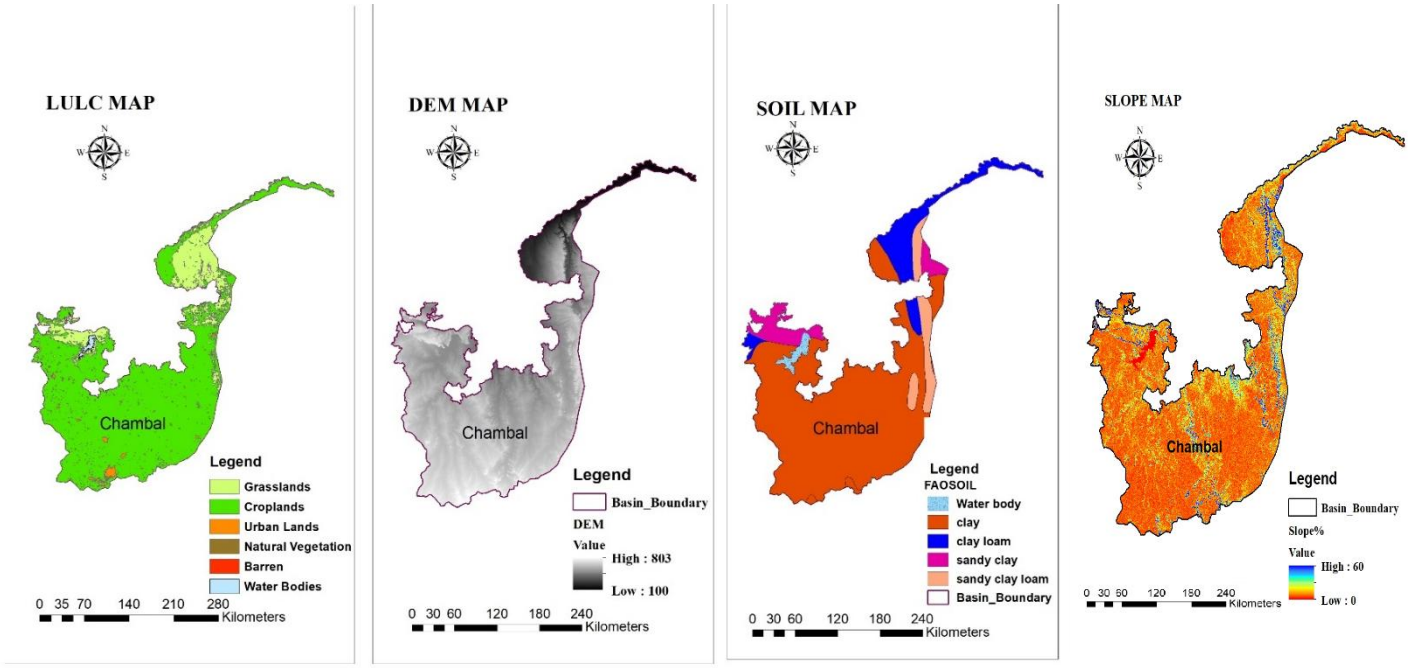

Fig.2: LULC map DEM map, Soil map, and slope map of Chambal basin in Madhya Pradesh

2.2 Methodology

The study employed the USLE and RUSLE models to assess spatially distributed soil erosion. The USLE, a basic empirical model, is extensively applied to estimate soil erosion in croplands with gently sloping terrain. The RUSLE, on the other hand, in several situations, including woodland, rangeland, and disturbed areas. In this example, some parameters have been enhanced with the updated essential characteristics (Belasri and Lakhouili, 2016). These models calculate the annual long-term soil loss rate in mass units per unit area by multiplying six primary parameters in a raster data format.

The following equation can be used to express the USLE and RUSLE models:

$$A=R*K*L*S*C*P \quad (1)$$

Where, A is the computed soil loss caused by rill and sheet erosion (t. ha-1. yr-1), R is the rainfall erosivity factor (MJ.mm.ha1.hr1.yr1), and K is the soil erodibility (t. ha.hr. $ha^{-1}.MJ^{-1}.mm^{-1}$), L is the Slope length factor (unitless), S is the slope steepness factor (dimensionless), C is the cover and management factor (unitless), and P is the Support practice factor (dimensionless). The conceptual framework for the USLE/RUSLE model's approximation of soil erosion is depicted in Fig. 3, and the steps for estimating various parameters in GIS context by creating thematic maps of these elements are shown below.

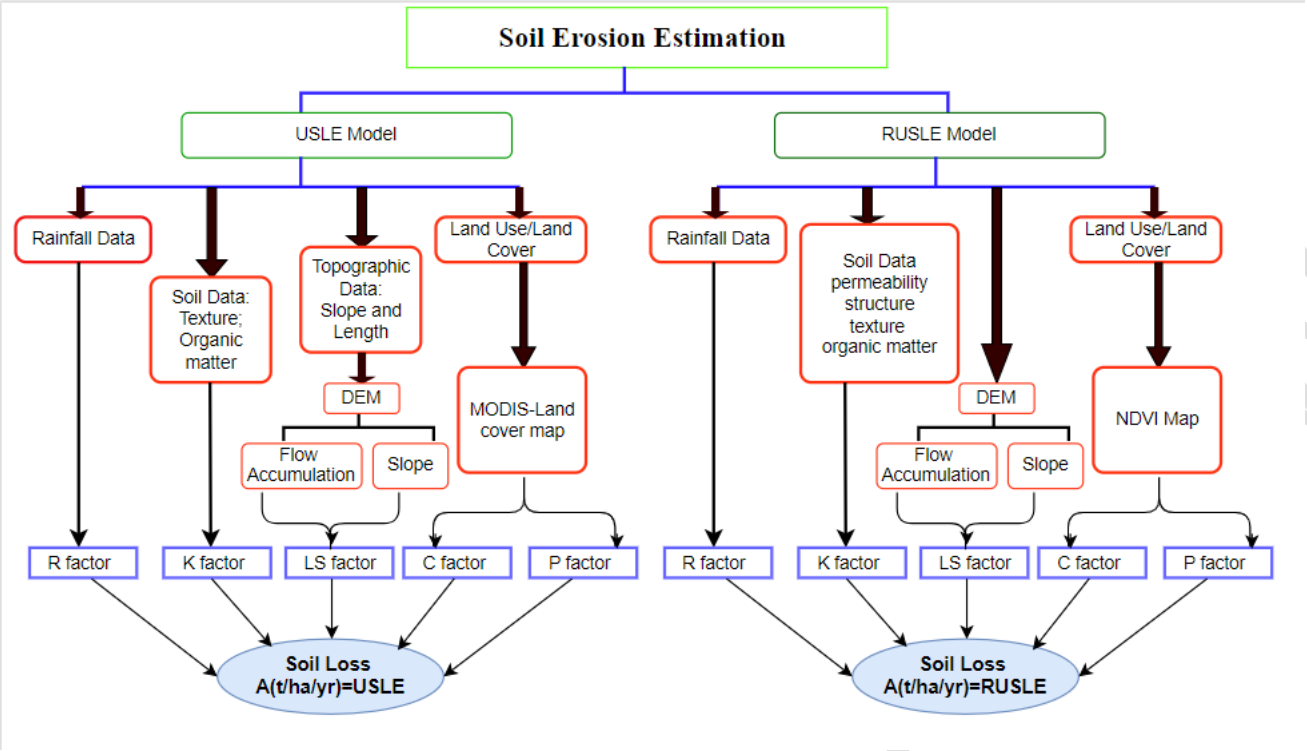

Fig 3. Conceptual workflow for analyzing soil loss using USLE and RUSLE models.

2.3 Database Creation for the USLE Model

2.3.1 Rainfall Erosivity Factor (R)

Rainfall erosivity(R) is the important variable to gauge the risk of soil erosion. One of the main variables used to gauge the risk for erosion is rainfall erosivity (R). For R factor estimate, Rambabu et al.'s empirical equation from 1979 was employed.
Data on annual rainfall for the past 20 years (1998–2018) was gathered in a raster format from CHIRPS (http://legacy.chg.ucsb.edu/data/index.html). The CHIRPS dataset was chosen in this investigation because it has superior geographical and temporal resolution and more recent data available than any other gridded dataset. Planetoid and ground-based Precipitation observations are combined in the CHIRPS datasets (Funk *et al,* 2015). The Chirps datasets for the Indian region have been used in several research (Divya and Shetty, 2021).

Applying the raster calculator module of QGIS and the ensuing formula, the R-factor was calculated:
$R = 22.8 + 0.64 * AAP$ ... (2)
Where R stands for rainfall erosivity factor and AAP for average annual precipitation, both in MJ.mm.ha.1.hr.1.yr1.

2.3.2 Factor of soil erodibility (K)

According to Khan *et al*. (2018), the soil erodibility factor is a measurement of a given soil's intrinsic erodibility under the standard conditions of the unit USLE plot, maintained in continuous fallow and tilled condition. Using Eq. (3), the K-factor map was created as follows:

KUSLE = Kw = fcl-si, forgc, fhisand, … *(3)*

Where, fcsand=Factor that raises the K indicator in soils with minimal sand and decreases it in soils with high coarse-sand content

For soils with high clay-to-silt ratios, fcl-si stands for low soil erodibility factors.

fhisand = Factor that decreases K values for soils with exceptionally high sand content, and forgc = Factor that lowers K values in soils with high organic carbon content.

Eqs. (4), (5), (6), and (7) can be used to calculate fcsand, fcl-si, forgc, and fhisand, respectively:

$$f_{csand}=\left(0.2+0.3\ exp\left[-0.256\ m_s\left(1-\frac{m_{silt}}{100}\right)\right]\right) \quad \ldots (4)$$

$$f_{cl\text{-}si}=\left(\frac{m_{silt}}{m_c+m_{silt}}\right)^{0.3} \quad \ldots (5)$$

$$f_{orgc}=\left(1-\frac{0.25\ orgC}{orgC+exp\left[3.72-2.95\ orgC\right]}\right) \quad \ldots (6)$$

$$f_{hisand}=\left(1-\frac{0.7\left(1-\frac{m_s}{100}\right)}{\left(1-\frac{m_s}{100}\right)+exp\left[-5.51+22.9\left(1-\frac{m_s}{100}\right)\right]}\right) \quad \ldots (7)$$

Where, ms=Sand fraction content (0.05-2.00 mm diameter), %, msilt=Silt fraction content (0.002-0.05 mm diameter), %, mc=Clay fraction content (<0.002 mm diameter),%, and orgC=Organic carbon (SOC) content,%.

2.3.3 Topographic Factor (LS)

The slope (S) and slope length (SL) factors consider topography when calculating how much soil erosion occurs. To determine the topographic component, elevation data through a digital elevation model (DEM) was used. To create only one topographic factor (LS), the L and S factors were first calculated independently (Wischmeier and Smith, 1965).

LS was determined by applying the Eq. (8) provided by Wischmeier and Smith (1965):

$$LS = (\sqrt{L}*0.305/\ 100) * (0.76 + 0.53*S + 0.076*S2) \quad \ldots (8)$$

Where S = Percent land slope, % and L = Field slope length, meters.
The topographical component was derived using QGIS's hydraulic tools.

2.3.4 Crop/Cover Management Factor (C)

The cropping management factor (C) is an estimate of the difference between soil loss from cultivated land under certain conditions and soil loss from clean tilled fallow on the same soil, slope, and rainfall conditions. According to the sowing and harvesting seasons in the area, this element reroutes the combined outcome of crop cover, crop sequence, and yield level, as well as the length of the growing season, tillage techniques, residue management, and the projected temporal distribution of erosive rainstorms (Warwade et al., 2014).

Table 2. C and P factor values for different Land use types

Sl. No.	Land use type	C-factor	P-factor
1.	Forest	0.001	1.00
2.	Agriculture/ Natural vegetation	0.128	0.92
3.	Grassland	0.003	1.00
4.	Urban	0.030	1.00
5.	Water body	0	1.00
6.	Barren land/wasteland	1.0	1.00

Source: Fernandez and Wu (2003)

Values of the C-factor (Table 2) as proposed by Fernandez and Wu (2003) were attributed to the LULC map in the current investigation. When the land was continuously bare fallow with no plant coverage (standard plot condition), the cover management factor (C) value was 1, and it was low when there was more vegetation or crop cover available since the low value led to reduced soil erosion. According to Fernandez and Wu (2003), the values of C for the forest, agriculture, grassland, urban, water body, and barren/wasteland were taken to be 0.001, 0.128, 0.003, 0.030, and 1 correspondingly.

2.3.5 Factor (P) for the Conservation/Support Practice

The ratio of soil erosion caused by a certain support practice to the corresponding soil erosion caused by up-slope and down-slope tillage is the basic definition of the support practice factor (P). As in the case of the C-factor for the USLE model, P-values were given in this study to the specific class of land use/land cover. The range of the P-factor value is 0 to 1. Table 2 displays the conservation/support practice factor (P) for various land uses and land covers. According to Fernandez and Wu (2003), the P-factor value is 0.92 for agriculture and 1 for all other land use types.

2.4 Development of Model Database for RUSLE

2.4.1 Rainfall Erosivity Factor (R)

The erosivity index and yearly rainfall were used to estimate the R-factor value for RUSLE, and Patil *et al*. (2017) also utilized this method to measure soil erosion:

$$Ra = 79 + 0.363 * Pa \ldots (9)$$

where Pa is the yearly rainfall average in millimeters.

2.4.2 Factor of Soil Erodibility (K)

The soil map that was acquired from the FAO website (www.fao.org) was used to create the K-factor map. The soil map offers details on permeability, organic content, and textural properties at various pixel levels. To determine the soil erodibility, these textural parameters were entered into the equation (10) proposed by Adhikary *et al*. (2014).

$$100\,K = 10^{-4} * 2.7\,1 * M^{1.14} * (12-a) + 4.2(b-2) + 3.23(c-3) \quad (10)$$

Where,
K = K-factor, (t.ha.hr. $ha^{-1}.MJ^{-1}.mm^{-1}$),
M = Texture from the first 150mm of soil surface = [(100−Ac) · (L+Armf)]
Ac = Percent of clay (< 0.002 mm),
L = Percent of silt (0.002–0.05 mm),
Armf= Percent of very fine sand (0.05–0.1 mm),
a = Percent of organic matter content,
b = Structure of soil (very fine granular=1, fine granular=2, coarse granular=3, lattic or massive=4); and
c = Permeability of soil (fast=1, fast to moderately fast=2, moderately fast =3, moderately fast to slow=4, slow=5, very slow=6).

Table 3. Estimated K-factor values of different soil series of Chambal basin

Sl. No.	Basin type	Soil type	Area, %	K-factor		b (Soil structure)	c (Soil permeability)
				USLE	RUSLE		
1.	Chambal	Clay	74.19	0.11	0.11	1	6
		Sandy clay loam	14.97	0.15	0.35	3	3
		Clay loam	6.64	0.14	0.30	2	4
		Sandy loam	2.06	0.16	0.54	3	2
		Sandy clay	1.76	0.13	0.20	2	5

2.4.3 (LS) Topographic Factor

If all other factors stay constant, the slope length factor (L) is the ratio of soil loss from a particular length of slope to land with a 22.12 m length of slope. If all other factors stay constant, the slope gradient factor (S) is the ratio of soil loss from a certain gradient of slope to that from land having a 9% slope (Warwade *et al*., 2014). The topographic factor (LS) is the combination of the L and S factors.

The following equation was created using the computed DEM and the topographic factor:

$$LS = (L / 22)^{0.5} * (0.065 + 0.045*S + 0.0065*S^2) \quad (11)$$

Where,
L = Field slope length, m, and
S = Percent land slope.

2.4.4 Crop/Cover Management Factor (C)

The C-factor, which describes situations that can be regulated the easiest to prevent erosion, is possibly the most important USLE/RUSLE factor. The primary biophysical indicator of soil erosion is the amount of vegetation cover. Using a seasonal image of 30 meters of resolution from the Normalized Difference Vegetation Index (NDVI), the C-factor in RUSLE was calculated.
The estimation of the C-factor utilized the following equation proposed by Van der *et al*. (2000)

$$C = \exp^{\left[-\alpha \frac{NDVI}{\beta - NDVI}\right]} \quad \ldots\ldots (12)$$

The α- values of 2 and 1, were used in the study, which produced promising outcomes. According to Kumar P. *et al.* (2012), C-factor values for well-protected soil ranged from 0 to 1 whereas those for bare soil were 1.

2.4.5 Conservation/ support practice factor (P)

Concerning the diverse cultivated area on earth, the support practice factor shows the soil loss rate. According to Gelagay and Minale (2016), the conservation practice factor for RUSLE is typically applied to disturbed landscapes and describes how management techniques including contouring, strip cropping, and terracing are utilized to prevent soil erosion. The P-factor value indicates how effective a conservation approach is at reducing soil erosion; the lower the P-factor value, the better the conservation technique is deemed to be at dropping erosion of soil. The P-factor value is 1 if no support practices are present. The P-factor value for RUSLE in this study ranges between 0.1 to 1.

2.5 Assessment of Annual Soil Erosion Rate

The annual average soil loss rate (A) occurring within the entire river basin was calculated using a combination of the RUSLE and USLE in QGIS 3.4. The QGIS 3.4 program was used to create, store, and evaluate raster layers of the R, K, LS, C, and P factors. The potential for simulated soil erosion for the entire state was calculated using this combination. Finally, the average yearly soil loss was calculated using equation (1) on a grid/cell basis, and the severity of soil erosion was rated for each grid/cell in the research region. To comprehend the soil erosion senior of the studied region, Mondal et al. (2016) also used these erosion categories.

The soil erosion results were validated from the studies conducted by Djoukbala *et al,*(2019) and Mondal *et al,*(2016) for an Algerian watershed and part of the Narmada River basin respectively, and it was observed that the RUSLE model gives a more trustworthy results as compared with the USLE of soil loss. The RUSLE model is regarded as the reference model for assessment of soil erosion in the current study because it was developed for an area predominately agricultural (Djoukbala *et al*., 2019), uses a revised equation over the USLE model for soil loss estimation, and uses NDVI data for this purpose (Mondal *et al*., 2016).

A study carried done at the Tucson, Arizona-based Southwest Watershed Research Centre of the USDA-ARS, demonstrates that the USLE and RUSLE estimates of soil loss were comparable for both yearly and average annual values. Both USLE and RUSLE had a propensity to underrate soil loss on fields with higher rates of erosion and overrate soil loss on fields with lower rates of erosion. According to Rapp *et al*. (2001), the crop cover and management element in RUSLE has the biggest impact on estimations of soil loss.

3. RESULTS AND DISCUSSION

3.1 Basin characteristics

The Chambal River basin, located in India, exhibits several fundamental characteristics of hydrological significance. The Chambal River, the principal river in this basin, is characterized by its perennial flow, originating from the Vindhyan Range. Furthermore, the Chambal River basin is notable for its unique topography, featuring steep ravines and gorges, which have been sculpted by the erosive power of the river over geological time. These features, along with their ecological significance, make the Chambal River basin an essential area for conservation and research in the field of hydrology and biodiversity.

Table 4. Characteristics details of Chambal River basin

Basin Name	Area (km^2)	River length (within state), km	Districts covered	Area under land covers, %	Area under various elevation (m) range, %

Chambal	59940	965	Sheopur, Guna, Rajgarh, Shajapur,Sehore, Agar malwa, Ujjain, Indore, Ratlam, Mandsour, Neemuch	15.34[1] 82.77[2] 1.29[3] 0.11[4] 0.47[5]	12.41[a] 89.96[b] 0.64[c]

Note: Land cover: 1 Forest, 2 Agriculture, 3 Urban,4 Fallow land, 5 Water body
Elevation: a 70-350 m, b 351-700 m, c 701-1317 m

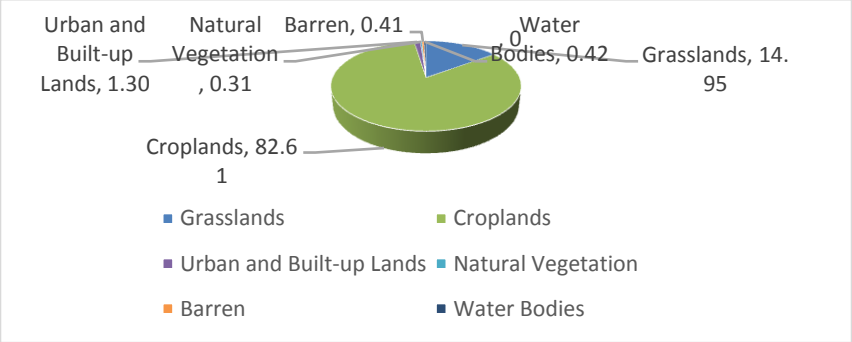

Fig.4: Pie chart showing the distribution of vegetation type.

Chambal River basin covers a total area of 59,940 km^2 and travels 965 km within Madhya Pradesh. From land cover study, it was observed that the basin area is maximum under agriculture (82%) followed by grassland (14.95%) in the river basin as shown in Table 4 and Figure 4 Topography of entire the basins under Chambal was further subdivided into three elevation categories and it was found that the river basin has a maximum area (90%) under highest elevation range between 350-1317 meter area.

3.2 Soil Erosion Using USLE

The average precipitation (rainfall) over the study basin was observed to range between 667.5mm to 1167.5 mm and the R-factor ranged from 450 to 770 MJ mm ha-1 hr-1 yr-1. The spatial variation and distribution of rainfall erosivity of the basin are depicted in Figure 5. Decreasing trend in R-factor was observed from north (770 mm ha-1 hr-1 yr-1) to south (450 mm ha-1 hr-1 yr-1) part of the basin. Soil triangle diagram was used to identify soil type based on percentage of sand, silt, and clay. The soil series, area under soil type, and K-factors values are presented in Table 3. The lower value of K-factor was found to be due to presence of shallow and medium deep soil (Kumari *et al*., 2019). The spatial variation of the slope (%) ranged from 0 to 60 as shown in figure 2 and topographic factor (LS factor) ranged from 0 to 98 across the entire basin for the USLE model illustrated in Figure 5.

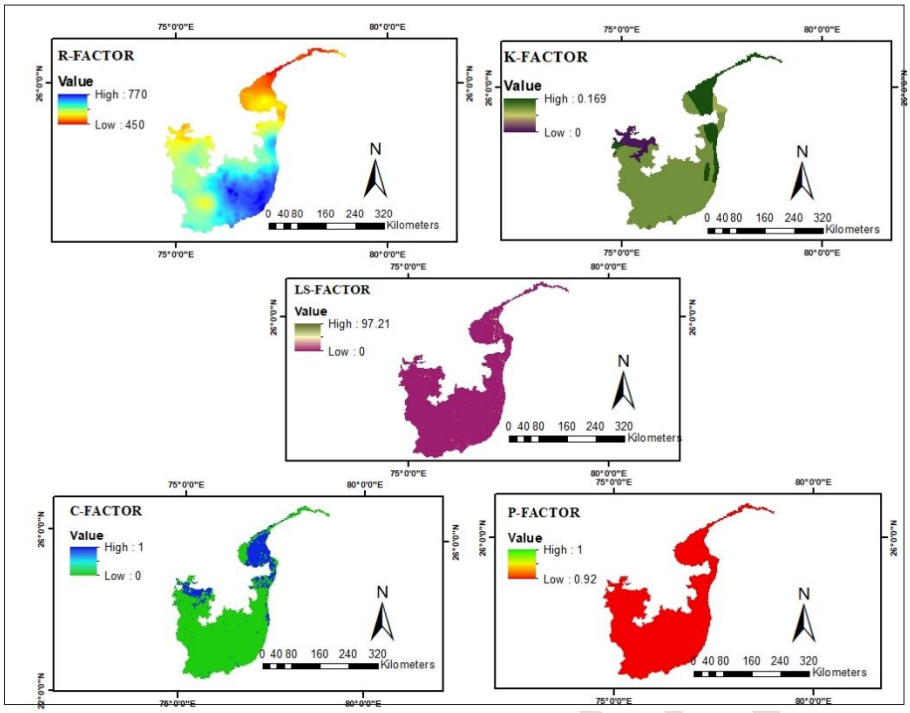

Fig. 5: Map showing spatial distribution of R, K, LS, C, and P-factor used in USLE models for Chambal basin.

The C-factor value for USLE model varies from 0 to 1, where the C-factor value is zero for healthy vegetation or dense forest area whereas for bare soil is 1. The P-factor value for Chambal basin ranges from 0.92 to 1.

3.3 Soil Erosion Estimation by RUSLE

From the spatial distribution of R-factor from the RUSLE model (figure 6), it was observed that the values ranged from 242.57 to 358.45 MJ mm ha-1 hr-1 yr-1 across the entire basin. The higher soil erodibility value (R-factor) of 0.54 was found to be in the Chambal basin/northern region and north-west part of the basin which can be attributed to the light textured soil found inthis region (figure 3).

The spatial distribution of K-factor, C-factor, LS factor, and P-factor are shown in figure 6. Soil erodibility was observed to be comparatively higher in the northern part of the basin than the southern region. The lowest soil erodibility in southern region is due to clay soil which is dominant soil type in this region. In northern region sandy soil, sandy clay, and clay loam are found in varying percentages which are more prone to erosion. The topographic factor (LS) ranged between 0 to 102.25 across the river basin for the RUSLE model. The C-factor spatial distribution map (Fig. 6) was developed using the relationship between NDVI and C-factor as given in Eq. 12. The C factor was found to have the lowest value (0) in the water body, the second lowest (0.001) forest, and the highest in barren land/wasteland (1).

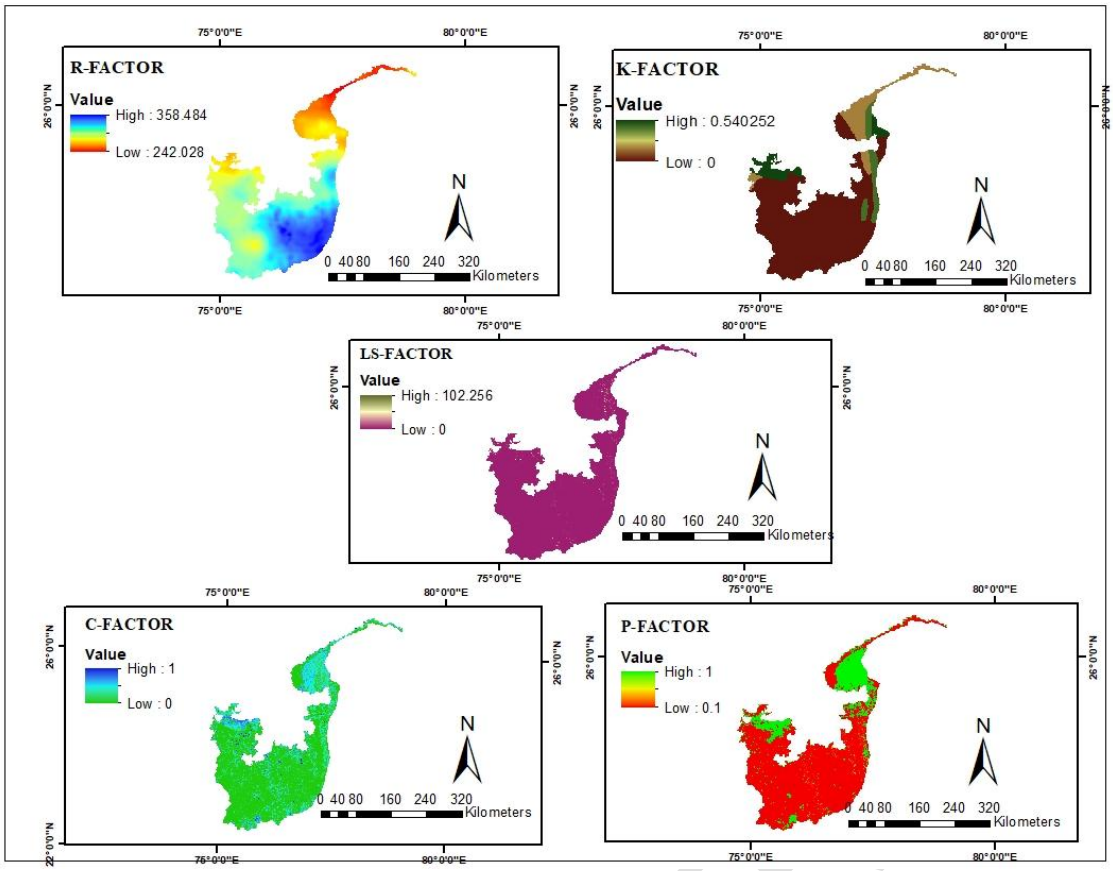

Fig. 6: Spatial map showing R, K, LS, C, and P-factor used in RUSLE models for Chambal basin.

4.4 Comparison of Rate of Soil Loss by Two Models

"Comparing the two models of RUSLE and USLE shows a similar pattern of soil loss. The USLE model of soil erosion revealed soil loss of less than 5 t. ha^{-1}. yr^{-1} (slight erosion) in the major area (94.67% of area), 20–40 t. ha^{-1}. yr^{-1} (very high) in 2.03%., 40–80 t. ha^{-1}. yr^{-1} (severe) in 0.33%, greater than 80 t. ha^{-1}. yr^{-1} (very severe) in 0.43% of area of the state. Similar results were obtained using RUSLE model with the major portion of the area (94.16% of area) being under less than 5 t. ha^{-1}. yr^{-1} (slight severity) category, 20–40 t. ha^{-1}. yr^{-1} (very high) in 1.15%, 40–80 t. ha^{-1}. yr^{-1} (severe) in 0.76%, greater than 80 t. ha^{-1}. yr^{-1} (very severe) in 0.78% of area of the state. Comparative analysis results of soil loss in the study area using different soil models are computed and tabulated in Table 5 and Figure 7. However, in both cases, soil type, vegetation, and elevation factors affected the rate of erosion". [49]

Table 5. Soil erosion rate group in USLE and RUSLE models.

S. No.	Class (t/ha/year)	USLE (km^2)	USLE (%)	RUSLE (km^2)	RUSLE (%)
1.	<5	53901.56	94.67	53737.40	94.19
2.	5 –10	1160.76	2.03	870.39	1.52
3.	10 –20	1006.73	1.76	898.28	1.57
4.	20 - 40	418.30	0.73	658.99	1.15
5.	40-80	188.14	0.33	438.90	0.76
6.	>80	260.77	0.45	445.99	0.78

The areas under different categories of soil erosion viz., moderate, normal, very high, extreme, and very severe rates were slightly higher in the RUSLE model than the area assessed by the USLE model (Table 5).Here, Table (6) specifies the average value of soil erosion for the complete basin is 2.0 t/ha/yr. and 3.04 t/ha/yr for USLE and RUSLE methods, correspondingly. It can be deciphered from Table (6) that the USLE model underestimated soil erosion when compared with the RUSLE model. Similar results were also reported by Mondal *et al*. (2016) for the part of the Narmada River basin where the USLE model underestimated soil erosion as compared to the RUSLE model.Kumar *et al*. (2022) reported an average annual soil loss of 1.60 t. ha^{-1}. yr^{-1} in the lower Chambal basin including Madhya Pradesh and Rajasthan part.

Table 6. Basic measurements.

S. No.	Method	Mean
1.	USLE	2.00
2.	RUSLE	3.04

The average values for both the methods are roughly the same. Therefore, in evaluation of both the models, the designed value of soil loss of RUSLE model was found to be nearest to the USLE model value. The soil loss computed by the RUSLE model is higher than the USLE model implying the impact of detailed soil information and NDVI based computation of factors for the RUSLE model. Hence, from the research study, it is recommended to prefer RUSLE model on availability of remote sensing data and soil information.

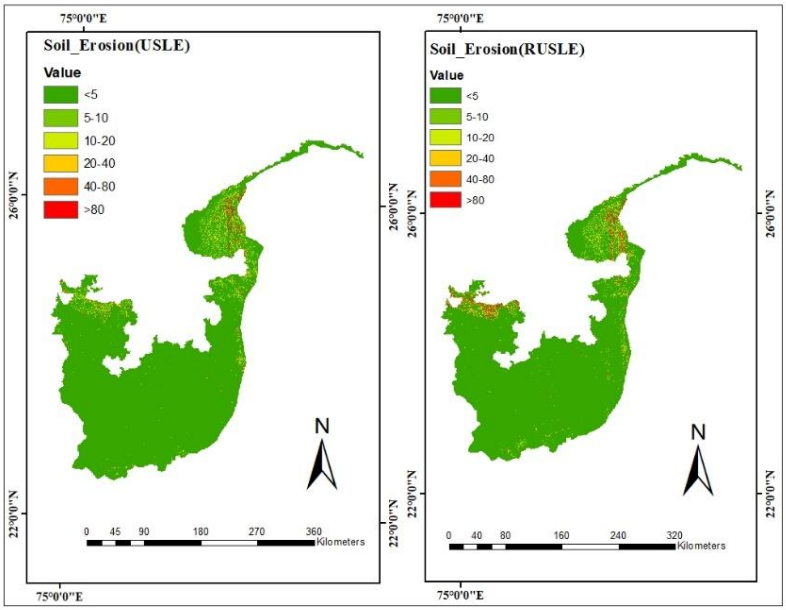

Fig.7: Soil erosion estimates (t. ha -1. yr-1) by USLE and RUSLE models for Chambal basin.

From the above table it is cleared that a major portion of the basin is degraded by erosion of (<5 t/ha/year) covering area 94.67% and 94.19% using USLE and RUSLE models, respectively. The percentage area comes under very sever class of erosion is 0.45% and 0.78% using USLE and RUSLE models, respectively. Bhind, Morena, Shivpuri, Sheopur, Neemach, and Mandsur are the districts that are facing the problem of severe soil erosion in the state of Madhya Pradesh.

5. CONCLUSION

The study on soil erosion conducted using the USLE and RUSLE models reveals the spatial distribution of erosion and identifies regions at the highest risk. The estimated average annual soil loss for the basin was 2.0 t. ha^{-1}. yr^{-1} according to the USLE model and 3.04 t. ha^{-1}. yr^{-1} according to the RUSLE model. In the USLE model, it was found that approximately 53,901.56 km^2 of the region experienced slight erosion, primarily in the Chambal basin. However, the USLE model also indicated that 0.45% of the area suffered from very severe erosion, 0.33% from severe erosion, and 0.73% from very high erosion. Likewise, the RUSLE model showed higher erosion rates, with 0.78% experiencing very severe erosion, 0.76% severe erosion, and 1.15% very high erosion. The study concluded that the most significant soil erosion occurred in the north-to-northwest margins of the basin, characterized by low vegetation and light soil. Substantial investments would be needed for the conservation of soil and water resources in areas with severe to very severe erosion. The USLE model

generally estimated lower soil loss compared to theRUSLE model, highlighting the impact of detailed soil data and NDVI-based factors in the RUSLE model. Therefore, the RUSLE model can be utilized for long-term soil loss assessment in agricultural watersheds in Madhya Pradesh when comprehensive soil information and remote sensing data are accessible.

REFERENCE

1. Adhikary P P, Tiwari S P; Mandal D; Lakaria B L; Madhu M. 2014. Geospatial comparison of four models to predict soil erodibility in a semi-arid region of Central India. *Environ. Earth Sci*.,72 (12), 5049–5062.http://dx.doi.org/10.1007/s12665-014-3374-7.

2. Amundson, R., Berhe, A. A., Hopmans, J. W., Olson, C., Sztein, A. E., & Sparks, D. L. 2015. Soil and Human Security in the 21st century. *Science*, *348*(6235), 1261071.https://pubmed.ncbi.nlm.nih.gov/25954014/

3. Biswas S. 2012. Estimation of soil erosion using remote sensing and GIS and prioritization of catchments. *Int. J. Emerging Technol. Adv. Eng*., 2 (7), 2250-2459.
4. https://www.researchgate.net/publication/300192067_Estimation_of_Soil_Erosion_using_Remote_Sensing_and_GIS_and_Prioritization_of_Catchments.

5. Belasri A, Lakhouili A. 2016. Estimation of soil erosion risk using the Universal Soil Loss Equation (USLE) and Geo-Information Technology in Oued El Makhazine watershed, Morocco. J. Geog. Info. Syst., 8, 98-107. http://dx.doi.org/10.4236/jgis.2016.81010

6. Divya P; Shetty A. 2021. Evaluation of CHIRPS satellite rainfall datasets over Kerala, India. Narasimhan M C; George V; Udaya Kumar G; and Kumar A (Eds.), Trends in Civil Engineering and Challenges for Sustainability, Lecture Notes in Civil Engineering, Springer, Singapore, 99, 655-664. http://dx.doi.org/10.1007/978-981-15-6828-2_49.

7. Djoukbala O; Hasbaia M; Benselama O; Mazour M. 2019. Comparison of the erosion prediction models from USLE, MUSLE and RUSLE in a Mediterranean watershed, case of Wadi Gazouana (NW of Algeria). Modell. *Earth Syst. Environ*., 5(2), 725-743.https://doi.org/10.1007/s40808-018-0562-6.

8. “Factual and Action Taken Report of Joint Committee Date of Visit: 17th May 2022 Location: National Chambal Sanctuary Stretch”, (2) (2022).
9. https://greentribunal.gov.in/sites/default/files/news_updates/Factual%20and%20Action%20Taken%20Report%20in%20OA%20No.%20248%20of%202022%20(In%20re%20News%20item%20published%20in%20The%20Hindu%20dated%2027.03.2022%20titled%20Digging%20up%20the%20Chambal).pdf

10. Fernandez C and Wu J Q. 2003. Estimating water erosion and sediment yield with GIS, RUSLE, and SEDD. J. Soil Water Conserv., 58 (3), 128-136.https://www.jswconline.org/content/58/3/128

11. Funk C; Peterson P; Landsfeld M; Pedreros D; Verdin J; Shukla S; Husak G; Rowland J; Harrison L; Hoell A; Michaelsen J. 2015. The climate hazards infrared precipitation with stations—A new environmental record for monitoring extremes. *Sci. Data*, 2 (1), 1-21. https://www.nature.com/articles/sdata201566

12. Gelagay A S; Minale H S. 2016. Soil loss estimation using GIS and Remote sensing techniques: A case of Koga watershed, Northwestern Ethiopia. *Int. Soil Water Consrv Res*., 4, 126–136.https://doi.org/10.1016/j.iswcr.2016.01.002.

13. IPCC 2017. Special Report on climate change, desertification, land degradation, sustainablelandmanagement,foodsecurity,andgreenhousegasfluxesinterrestrialecosystems(SR2).*IntergovernmentalPanelon ClimateChange*(IssueFebruary).

14. IPCC, 2022: Climate Change 2022: Impacts, Adaptation and Vulnerability. Contribution of Working Group II to the Sixth Assessment Report of the Intergovernmental Panel on Climate Change. Pörtner H O, Roberts D C, TignorM,. Poloczanska E S, Mintenbeck K, Alegría A, Craig M, Langsdorf M, Löschke S, Möller, A. Okem, B. Rama (eds.)]. Cambridge University Press. Cambridge University Press, Cambridge, UK and New York, NY, USA, 3056 pp., http://dx.doi.org/10.1017/9781009325844.

15. ISRO,D.2016.LandDegradationAtlasofIndia.SpaceApplicationsCentre,ISRO,Ahmedabad.

16. Joshi V U 2014 The Chambal Badlands; In: Landscapes and Landforms of India (ed.) Kale V S, Springer, Netherlands, pp. 143–149. https://doi.org/10.1007/978-94-017-8029-2˙13.(I couldn't find the source)

17. Kar, S. K., Kumar, S., Sankar, M., Patra, S., Singh, R. M., Shrimali, S. S., & Ojasvi, P. R. (2022). Process-based modelling of soil erosion: scope and limitation in the Indian context. *Current Science*, *122*(5), 533-541.(I couldn't find the source)

18. Kaushik, P., Ghosh, P. (2015). Geomorphic evolution of Chambal River origin in Madhya Pradesh using remote sensing and GIS. *Int J Adv Remote Sens GIS*, *4*(1), 1130-1141.http://dx.doi.org/10.23953/cloud.ijarsg.127.

19. Khose, S. B., Mailapalli, D. R., Biswal, S., & Chatterjee, C. (2022). UAV-based multispectral image analytics for generating crop coefficient maps for rice. *Arabian Journal of Geosciences*, *15*(22), 1681.http://dx.doi.org/10.1007/s12517-022-10961-2.

20. Khose, S., & Rao Mailapalli, D. (2023, May). Prediction of Surface Soil Moisture Content using Multispectral Remote Sensing and Machine Learning. In EGU General Assembly Conference Abstracts (pp. EGU-7778).http://dx.doi.org/10.5194/egusphere-egu23-7778.

21. Khose, S. B., Dhokale, K. B., & Shekhar, S. (2023b). The Role of Precision Farming in Sustainable Agriculture: Advancements and Impacts.
22. https://www.researchgate.net/publication/373166415_The_Role_of_Precision_Farming_in_Sustainable_Agriculture_Advancements_and_Impacts_Article.

23. Khose, S., Biswal, S., Mailapalli, D., Chatterjee, C. 2021. Application of UAV in Estimation of Crop Coefficient (Kc) using Field and Remote Sensing Data. In AGU Fall Meeting Abstracts (Vol. 2021, pp. H35T-1269).http://dx.doi.org/10.1002/essoar.10510761.1.

24. Khan S; Singh A; Bhadauria S S; Yadav S S; Sharma A. 2018. Soil loss estimation of a watershed of central India with integration of geospatial techniques and universal soil loss equation. *Int. J. Agric. Environ. Biotechnol*., 11(4), 703-711. http://dx.doi.org/10.18393/ejss.288350.

25. Kumar S, M. Sankar, S. Patra, R. M. Singh, S. S. Shrimali ,P. R. Ojasvi. 2022 Process-based modelling of soil erosion: scope and limitation in the Indian context *Current Science*, 122, NO. 5. http://dx.doi.org/10.18520/cs/v122/i5/533-541.

26. Kottek M, Grieser J, Beck C, Rudolf B, Rubel F. 2006. World Map of the Köppen-Geiger climate classification updated. Meteorologische Zeitschrift. 15:259–263.http://dx.doi.org/10.1127/0941-2948/2006/0130.

27. Kumar, R., Devrani, R., & Deshmukh, B. 2022. A Review of Remote Sensing and GIS-Based Soil Loss Models with a Comparative Study from the Upper and Marginal Ganga River Basin. *Advances in Remote Sensing Technology and the Three Poles*, 321-339.http://dx.doi.org/10.1002/9781119787754.ch22.

28. Lal, R., 2003. Soil erosion and the global carbon budget. Environ. Int. 29(4), 437–450.https://doi.org/10.1016/S0160-4120(02)00192-7.

29. Maji, A. K., Reddy, G. O., Sarkar, D., 2010. Degraded and waste lands of India: status and spatial distribution. Indian Council of Agricultural Research and National Academy of Agricultural Science, New Delhi, p. 158.https://www.researchgate.net/publication/322222168_Degraded_and_Wastelands_of_India_Status_and_Spatial_Distribution.

30. Marcinkowski, P., Szporak-Wasilewska, S., Kardel, I. (2022). Assessment of soil erosion under long-term projections of climate change in Poland. *Journal of Hydrology*, *607*, 127468.https://doi.org/10.1016/j.jhydrol.2022.127468.

31. Mitasova, H., Barton, C. M., Ullah, I., Hofierka, J., Harmon, R. S. (2013). GIS-based soil erosion modeling. In *Remote Sensing and GIScience in Geomorphology* (pp. 228-258).http://dx.doi.org/10.1016/B978-0-12-374739-6.00052-X.

32. Morgan, R.P.C.; Morgan, D.D.V.; Finney, H.J. A predictive model for the assessment of soil erosion risk. *J. Agric. Eng. Res.* **1984**, *30*, 245–253. https://doi.org/10.1016/S0021-8634(84)80025-6

33. Mondal A; Khare D; Kundu S. 2016. A comparative study of soil erosion modelling by MMF, USLE and RUSLE. *Geocarto Int*., 33(1), 89-103.http://dx.doi.org/10.1080/10106049.2016.1232313.

34. Pani P and Paul Carling P, 2013. Land degradation and spatial vulnerabilities: a study of inter-village differences in Chambal Valley, India, Asian Geographer, 30:1, 65-79, https://doi.org/10.1080/10225706.2012.754775.

35. Pani P, 2022. Progress in Indian Geography: A Country Report, 2016-2022. The 34th The Extraordinary Centennial Congress, IGU, Paris, France (July 18-22, 2022). Indian National Science Academy, New Delhi.

36. Patil R J; Sharma S K; Tignath S; Sharma A P M. 2017. Use of remote sensing, GIS and C++ for soil erosion assessment in the Shakkar River basin, India. Hydrol. Sci. J., 62(2), 217-231.https://doi.org/10.1080/02626667.2016.1217413.

37. Prakash S. 2019. Performance assessment of CHIRPS, MSWEP, SM2RAIN-CCI, and TMPA precipitation products across India. J. Hydrol., 571, 50-59. https://doi.org/10.1016/j.jhydrol.2019.01.036.

38. Rapp J F; Lopes V L; Renard K G. 2001. Comparing Soil Erosion Estimates from RUSLE and USLE on Natural Runoff Plots. In: Ascough J CII; Flanagan D C (Eds.), Soil Erosion Research for the 21st Century, Proc. *Int. Symp., Honolulu, HI, St. Joseph, USA*, MI: ASAE.701P0007, 24-27.
39. https://www.researchgate.net/publication/313658818_Comparing_soil_erosion_estimates_from_RUSLE_and_USLE_on_natural_runoff_plots.

40. Ritu Kumari, Pratibha Kumari, Reena Kumari and Veerendra K. Chandola. 2019. Growth and Yield Responses of Soybean under Rainfed Condition in Selected Districts of Madhya Pradesh,India.*Int.J.Curr.Microbiol.App.Sci*. 8(8): 713-721. https://doi.org/10.20546/ijcmas.2019.808.081

41. Sakinatu I, Ashraf M A, 2017. Impact of soil erosion and degradation on water quality: a review, *Geology, Ecology, and Landscapes,* 1:1, 111. http://dx.doi.org/10.1080/24749508.2017.1301053.

42. Senapati, U., Das, T. K. 2020. Assessment of potential land degradation in Akarsa Watershed, West Bengal, using GIS and multi-influencing factor technique. *Gully Erosion Studies from India and Surrounding Regions*, 187-205.http://dx.doi.org/10.1007/978-3-030-23243-6_11.

43. Suryawanshi, A., Nema, A. K., Jaiswal, R. K., Jain, S., Kar, S. K., 2021. Identification of soil erosion prone areas of Madhya Pradesh using USLE/RUSLE. *J Agri Engg*, *58*(2), 177-191.
44. http://dx.doi.org/10.52151/jae2021581.1744.

45. Ranga V, Van Rompaey A, Poesen J, Mohapatra S.N., Pani P., 2015. Semi-automatic delineation of badlands using contrast in vegetation activity: a case study in the lower Chambal valley, India, Geocarto International, 30:8, 919-936. http://dx.doi.org/10.1080/10106049.2015.1004130.

46. Van der Knijff J M; Jones R J A and Montanarella L. 2000. Soil Erosion Risk Assessment in Europe. European Soil Bureau- Joint Research Centre, EUR 19044 EN, Office for Official Publications of the European Communities, Luxembourg, pp: 34. https://www.unisdr.org/files/1581_ereurnew2.pdf.

47. Warwade P; Hardaha M K; Kumar D; Chadniha S K. 2014. Estimation of soil erosion and crop suitability for a watershed through remote sensing and GIS approach. Indian J. Agric. Sci., 84(1), 18-23. https://doi.org/10.56093/ijas.v84i1.37140.

48. Wischmeier W H; Smith D D. 1965. Predicting Rainfall Erosion Losses from Cropland East of the Rocky Mountains. U.S. Department of Agriculture Science and Education Administration, Washington, DC, USA, Agriculture Handbook No. 282, pp: 47

49. Mohod AG, Khandetod YP. Thermal analysis of solar tunnel dryer and evaluation for commercial mango leather drying. Journal of Agricultural Engineering. 2021;58(1):90-100.

DEFINITIONS, ACRONYMS, ABBREVIATIONS

Here is the Definitions section. This is an optional section.

Term: Definition for the term